Layer Stripping FWI for Surface Waves

Isabella Masoni, Total E&P , R. Brossier, University Grenoble Alpes, J. L. Boelle, Total E&P, J. Virieux, University Grenoble Alpes*

SUMMARY

In this study, an innovative layer stripping approach for FWI specifically adapted to the physics of surface waves is investigated, to mitigate the cycle skipping problem. A combined high-to-low frequency filtering with gradually increasing offset ranges, are applied to observed and calculated data to update gradually deeper layers of the shear velocity model. Successful results for a synthetic data example are presented.

INTRODUCTION

The construction of subsurface velocity models is an ongoing issue for oil and gas exploration. For land and shallow marine acquisitions, topography and weathered or unconsolidated top layers can lead to a very complex near surface, that can cause problems for the imaging of deeper exploration targets due to the presence of groundroll. In such cases, an innovative characterization of near surface properties is needed. Surface waves, conventionally considered as noise, sample this shallow zone, and may provide information on the velocity heterogeneities present. As a high-resolution imaging technique, waveform inversion allows extension beyond the locally layered assumption of conventional surface wave imaging methods.

MOTIVATION

The generic FWI formalism does not rely on a specific wave type. In practice however, success with FWI has mainly exploited body waves under an acoustic approximation of wave-propagation. Although some elastic FWI applications have been performed using body waves, the use of surface waves is still challenging (Brossier et al., 2009).

When considering slow surface waves propagating in the low velocity medium of the near surface, finding a sufficiently accurate initial model is essential for avoiding local minima. If the initial data do not predict the observed data with an error smaller than half a period, the optimization goes to a local minimum due to cycle-skipping (Mulder and Plessix, 2008).

One way to tackle this issue is to implement more robust misfit functions, such as an envelope misfit (Yuan et al., 2015), or taking advantage of alternative data domains (Pérez Solano et al., 2014; Masoni et al., 2014). In addition multiscale approaches such as wavelet decomposition (Yuan et al., 2015) or conventional frequency continuation approachs (Bunks et al., 1995; Sirgue and Pratt, 2004), are used to invert low-to-high frequency content, updating first the large-scale structure, and then the more detailed features of the velocity model.

This study investigates an innovative layer stripping approach for FWI specifically adapted to the physics of surface waves. Layer stripping is a well known approach used in inversion methods (Gibson et al., 2009; Shi et al., 2015), in which the model is recovered layer by layer in a top-to-bottom manner. The frequency content of surface waves is directly related to their penetration depth. Surface waves of higher frequency and shorter wavelength will therefore sample the top layers of a medium, while waves with lower frequencies and longer wavelengths will sample as well deeper parts of a medium. This can be observed by analyzing frequency gradients (Figure 1). This suggests an inversion workflow from high-to-low frequency content, leading to a layer-stripping FWI approach.

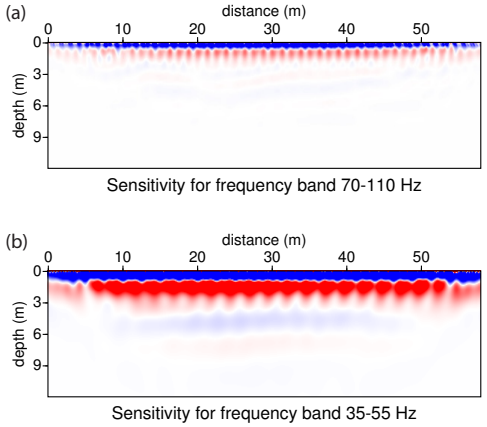

Figure 1: Data gradients over frequency bands $70-110\ Hz$ (a) and $35-55\ Hz$ (b). One can observe that lower frequency band samples the model at greater depths, but it is also of lower resolution (same color scale used for (a) and (b)).

In this study, the synthetic model from Pérez Solano et al. (2014) (Figure 6d) is used to test and evaluate layer stripping FWI for surface waves. The S-wave and P-wave velocity models are related by a constant poisson ratio (VP/VS = 2.0), with a homogeneous density model of $\rho = 1000\ kgm^{-3}$. Two high velocity anomalies, at the center of the model, are the targets of the inversion. Elastic 2D wave propagation is simulated using a finite difference method. The synthetic data (Figure 5a) is recorded by 145 vertical and horizontal component receivers, at 0.2 m below the surface. 20 vertical sources, positioned 0.2 m below the surface are simulated using a 40 Hz Ricker as the source wavelet. The initial shear velocity model consists of a linear gradient (Figure 4), and is the only parameter to be inverted. The true P-wave and density models, as well as the true source signature, are used. The focus is on the exploitation of the surface waves, which dominate the data in amplitude and are the main wavefield component driving misfit minimization. These contain information on the shear velocity properties of the medium. The initial data is heavily cycle-skipped (Figures

5b and 5c), and conventional FWI does not allow convergence.

LAYER STRIPPING FWI

For layer stripping FWI a high-to-low frequency filtering strategy is combined with gradually increasing offset ranges, to update gradually deeper layers of the shear velocity model.

Observed and calculated data are first windowed in offset, enforcing the layer stripping approach, and focusing only on surface waves that contain information on the layer to be updated. The limited offsets also reduce the dependence on the initial model, helping to avoid cycle-skipping. The maximum offset length is determined as a function of the penetration depth, estimated as equivalent to one wavelength. For the model considered, suitable offset ranges where calculated as

$$x_{max} \simeq 5\bar{\lambda}_S, \text{where} \quad \bar{\lambda}_S \simeq \frac{\bar{V}_S}{\bar{f}}, \tag{1}$$

using the average frequency $\bar{f}$ of the frequency band and the average shear velocity $\bar{V}_S$ of the depth layer of the initial model for each frequency band step.

The frequency spectrum of the data is then whitened and band-pass filtered. Larger frequency windows are selected for the initial high frequency bands, for which the frequency spectrum of the data has low amplitudes (Figure 2). The frequency bands are more tightly sampled where one can expect a better illumination of the velocity model. The layer stripping technique does not rely on the low frequency content of the data, often missing, to converge.

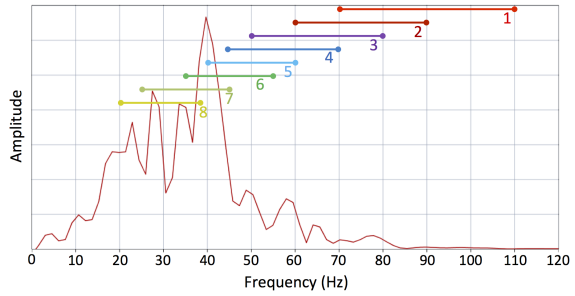

Figure 2: Frequency spectrum of the observed data. Frequency band ranges for layer stripping FWI steps (1-8) corresponding to the result in Figure 4 are superimposed on the graph.

The data misfit is obtained using either the conventional L2 norm of the difference, or the robust misfit function in the frequency-wavenumber (ω,k) domain (Masoni et al., 2014). The formulations of the two misfit functions are given as

$$C_{t,x} = \frac{1}{2}\sum_S \sum_R \mathbf{w}_R \left(\mathbf{d}_{obs}(t,x) - \mathbf{d}_{cal}(t,x)\right)^2, \tag{2}$$

and

$$C_{\omega,k} = \frac{1}{2}\sum_S \sum_R \mathbf{w}_R \left(|\,\mathbf{d}_{obs}(\omega,k)| - |\,\mathbf{d}_{cal}(\omega,k)|\,\right)^2, \tag{3}$$

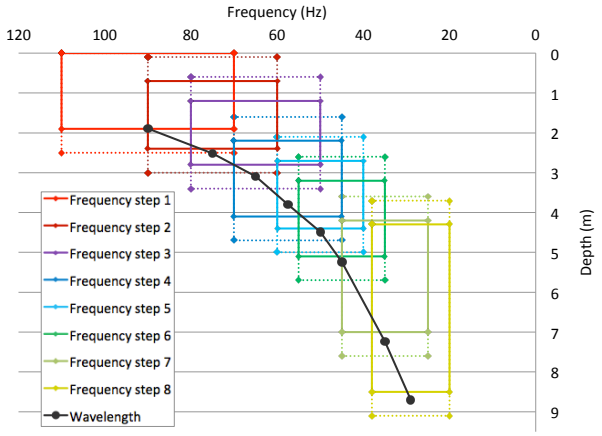

Figure 3: Plot of frequency band against depth window used for layer stripping FWI to produce the result in Figure 4. Each color corresponds to a frequency band inversion step, the dotted lines correspond to the depth window taper extent. The estimated average wavelength is plotted in black.

where $\mathbf{w}_R$ is the weighting applied for windowing in offset.

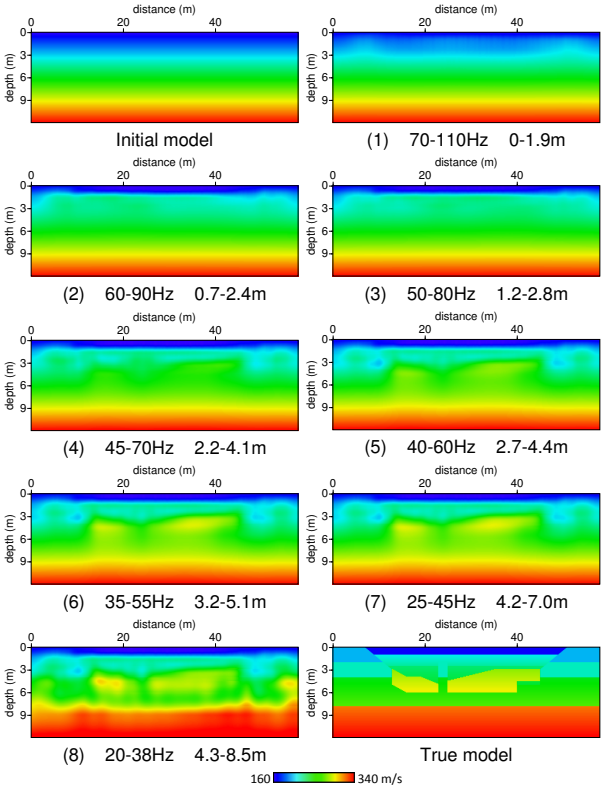

Figure 4: Evolution of the shear velocity model at each frequency band step (1-8) when using the conventional L2 norm of the difference in the (t,x) domain. The model is updated in a top-to-bottom manner, using a high-to-low frequency approach. The initial and true shear velocity models are also shown for reference.

The gradient is then calculated using the adjoint-state method (Chavent, 1974; Plessix, 2006), but only within a depth range chosen to correspond to the frequency band used. The top of the model update is frozen to avoid reducing the resolution previously obtained with higher frequency data, and the maximum depth is defined by the penetration limit of the surface waves (Figure 3).

The main pitfall for layer stripping FWI is finding the correct relation between the frequency bands and the depth windows, which utimately depends on the unknown velocity model. A good estimation of the penetration depth can be obtained from sensitivity kernels. Furthermore the sensitivity of the depth window can be reduced by applying a significant tapering (Figure 3), which greatly improves the quality of the results.

A depth preconditioned l-BFGS optimization is used for the inversion. This partially compensates for the decrease of surface wave amplitudes with depth (Plessix and Mulder, 2008; Pérez Solano, 2013). The final result of each frequency band is used as the initial model for the following one. Figure 4 shows the shear velocity model at each step of the layer stripping inversion when implementing the conventional L2 misfit function in the (t,x) domain.

RESULTS

Tests for layer stripping FWI are performed using both conventional (t,x) domain as well as (ω,k) domain misfit functions.

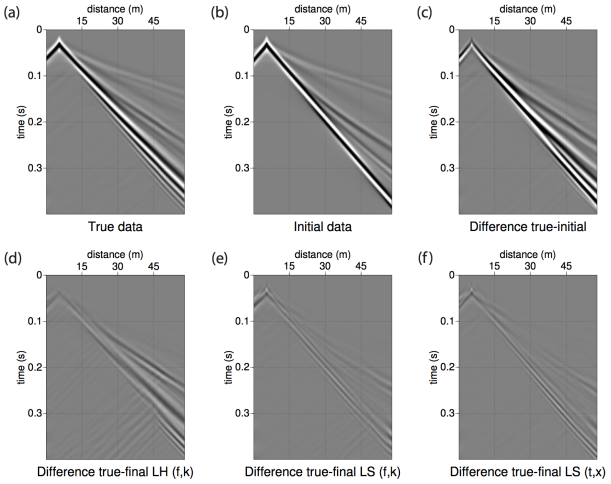

Figure 5: Common shot gather for the true data (a); initial data (b); difference true-initial (c); and the difference true-final after multiscale FWI with an (ω,k) domain misfit function (d); after layer stripping FWI with an (ω,k) misfit (e); and after layer stripping FWI with an (t,x) misfit (f).

These are compared to the result from conventional multiscale FWI, implementing increasing frequency bands with a low-cut frequency of 10 Hz and high-cut frequencies of 18 Hz, 25 Hz, 36 Hz, 50 Hz, 80 Hz and 110 Hz. The (ω,k) domain misfit function has already been shown to be more robust for this approach (Pérez Solano et al., 2014) and is therefore used, and the whole depth of the model is updated during each step. All other FWI parameters are kept constant at the true values.

The final velocity models are compared in Figure 6, and the corresponding data in Figure 5. One can observe that layer stripping FWI converges towards the true model for both tested misfit functions, and the final data residual is smaller than the one obtained by multiscale FWI. It is interesting to note that the data residual after multiscale FWI has a lower frequency content, suggesting that large scale features of the model are not fully recovered.

The layer stripping strategy does not inherently overcome the cycle-skipping limitations during inversion: the related data selection (frequency-offset) and the gradient windowing associated with the physics of surface waves reduce the dependence on the initial model. These windowings are crucial to avoid cycle-skipped data, allowing convergence.

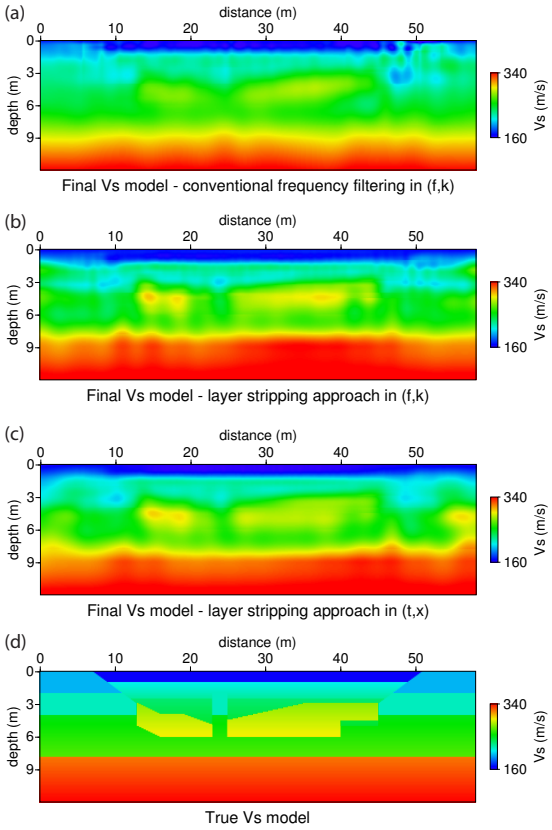

Figure 6: Comparison of final shear velocity models obtained after multiscale FWI (low-to-high frequency) and the (ω,k) domain misfit function (a); layer stripping FWI and the (ω,k) domain misfit function (b); layer stripping FWI and the conventional (t,x) domain misfit function (c); and the true shear velocity model (d).

For an objective quality control on the inversion results, the conventional (t,x) domain misfit between the observed data and the final data obtained after each frequency band step during FWI are plotted in Figure 7, regardless the misfit used for

the optimization. Multiscale FWI reduces the data misfit by less than 5 percent of the initial value, while a better performance is achieved by layer stripping FWI, which reduces the misfit by less then 1 percent. **It is interesting to note that the local minima issue is overcome during multiscale FWI when considering the (ω,k) domain misfit function. Je ne comprends pas...**

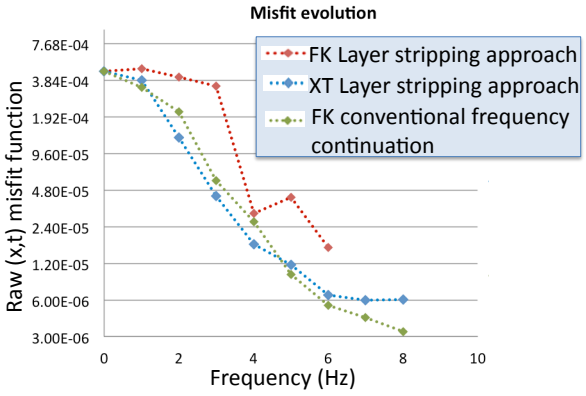

Figure 7: The conventional (t,x) domain misfit is used to calculate the difference between the true data, and the data corresponding to the final model obtained for each frequency band step, to provide a misfit evolution. The misfit evolution for both multiscale FWI (red) and layer stripping FWI (blue and green) are plotted.

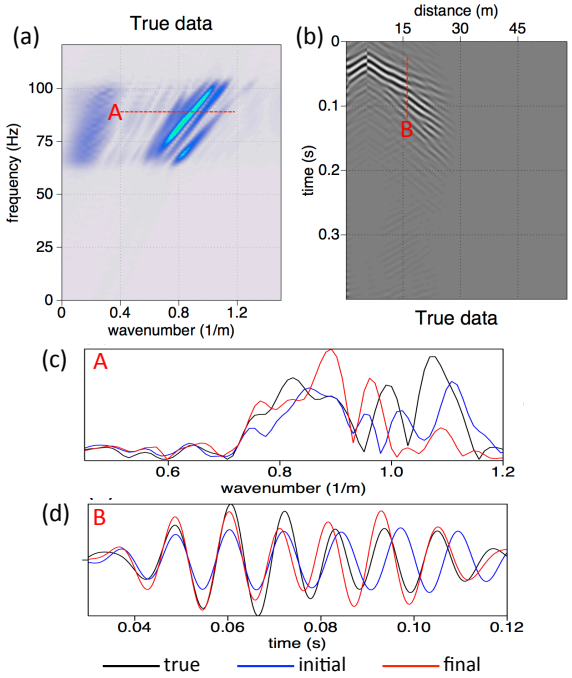

Figure 8: Comparison of data, at the moment when the misfit is computed during the first frequency band, for the (ω,k) domain misfit function (a) and the (t,x) domain misfit function (b). An example trace for the true, initial and final data are plotted in (c) and (d) respectively. The chosen traces are marked in red.

FURTHER ANALYSIS

Further tests are performed with layer stripping FWI to compare the robustness of the conventional (t,x) domain misfit function to the (ω,k) domain misfit function. For example, using a wrong relation between the frequency bands and depth windows chosen may prevent convergence. Although the test results are not shown here, the (ω,k) domain misfit function appears less successful for layer stripping FWI, and instabilities due to cycle-skipping occur.

The selection of high frequencies at the beginning of the inversion, and the whitening of the frequency spectrum, makes the role of complex higher modes important in the calculation of the misfit (Figure 8a), which may lead to cycle-skipping problems (Figure 8c). Instead the (t,x) domain misfit function appears to behave robustly and produce successful results.

CONCLUSIONS

Our study proposes a new layer stripping strategy to overcome cycle skipping problems for FWI when considering surface waves which have low speeds. The combined high-to-low frequency filtering with gradually increasing offset ranges update gradually deeper layers of the shear velocity model successfully, using the inherent localized sampling of surface waves near the free surface as shown on a synthetic data example. The robustness of the method allows the use of the conventional (t,x) domain misfit function, and appears to converge better than conventional multiscale FWI using the robust (ω,k) domain misfit function. Furthermore, layer stripping FWI does not rely on the existence of low frequency content of the data to converge.

The next step will be the application to a real dataset.

ACKNOWLEDGMENTS

The authors would like to thank TOTAL E&P for permission to show these results. We also thank Pérez Solano et al. (2014) for permission to use their synthetic model. This study was partially funded by the SEISCOPE consortium (*seiscope2.osug.fr*).

REFERENCES

Brossier, R., S. Operto, and J. Virieux, 2009, Seismic imaging of complex onshore structures by 2D elastic frequency-domain full-waveform inversion: Geophysics, **74**, WCC105–WCC118.

Bunks, C., F. M. Salek, S. Zaleski, and G. Chavent, 1995, Multiscale seismic waveform inversion: Geophysics, **60**, 1457–1473.

Chavent, G., 1974, Identification of parameter distributed systems, *in* Identification of function parameters in partial differential equations: American Society of Mechanical Engineers, New York, 31–48.

Gibson, B., M. Odegard, and G. Sutton, 2009, Nonlinear least-squares inversion of traveltime data for a linear velocity-depth relationship: Geophysics, **44**, 185–194.

Masoni, I., R. Brossier, J.-L. Boelle, M. Macquet, and J. Virieux, 2014, Robust full waveform inversion of surface waves: Seismic Technology, **11**, 19.

Mulder, W., and R. E. Plessix, 2008, Exploring some issues in acoustic full waveform inversion: Geophysical Prospecting, **56**, 827–841.

Pérez Solano, C., 2013, Two-dimensional near-surface seismic imaging with surface waves: alternative methodology for waveform inversion: PhD thesis, École Nationale Supérieure des Mines de Paris.

Pérez Solano, C., D. Donno, and H. Chauris, 2014, Alternative waveform inversion for surface wave analysis in 2-d media: Geophysical Journal international, **198**, 1359–1372.

Plessix, R. E., 2006, A review of the adjoint-state method for computing the gradient of a functional with geophysical applications: Geophysical Journal International, **167**, 495–503.

Plessix, R. E., and W. A. Mulder, 2008, Resistivity imaging with controlled-source electromagnetic data: depth and data weighting: Inverse Problems, **24**, 034012.

Shi, T., J. Zhang, Z. Huang, and C. Jin, 2015, A layer-stripping method for 3D near-surface velocity model building using seismic first-arrival times: Journal of Earth Science, **26**, 502–507.

Sirgue, L., and R. G. Pratt, 2004, Efficient waveform inversion and imaging : a strategy for selecting temporal frequencies: Geophysics, **69**, 231–248.

Yuan, Y., F. Simons, and E. Bozdag, 2015, Multiscale adjoint waveform tomography for surface and body waves: Geophysics, **80**, no. 5, R281–R302.